

A Compact Broadband Dual-Polarized Antenna for OTA Testing of Sub-6 GHz 5G New Radio

P. Singh^{1,*}, F.H. Ali^{2,†}

¹ Department of Test and Measurement, Rohde & Schwarz., New Delhi, India

² School of Engineering and Informatics, University of Sussex., United Kingdom

(Received 05 September 2023; revised manuscript received 14 December 2023; published online 27 December 2023)

The implementation of antenna arrays, beamforming, and millimeter-wave communication in a 5G network requires a novel approach to testing the radio performance of the devices. Over-the-air testing is a practical solution for measuring the radio performance of next-generation wireless systems. This paper presents the analysis and design of the dual-polarized Vivaldi antenna for over-the-air testing of a 5G base station for the frequency range spanning from 1.4 GHz to 6 GHz. The designed antenna consists of two elements arranged in an orthogonal fashion. The two dual-polarized Vivaldi antenna prototypes are modeled: one with an offset between the antenna elements and the other without an offset between the antenna elements. The wideband antenna is mainly characterized by an acceptable reflection coefficient (S11) over the desired operational bandwidth. The simulation results show S11 less than -10 dB across 1.4 to 6 GHz frequency range in both prototypes. The CST Studio Suite EM simulator is used to create and simulate the proposed antenna utilizing the Rogers RO4350B substrate, which has an overall size of $86 \times 90 \times 0.5$ mm³. The proposed antenna will be used at the UE side inside the anechoic chamber to test 5G base station over the air in terms of throughput and mobility. The compact size and low cost are the key features of this antenna. Low cost is achieved by using cheap dielectric material.

Keywords: Beamforming, Dual-polarization, Over-the-Air testing, Radiation pattern, Return loss, Vivaldi antenna.

DOI: [10.21272/jnep.15\(6\).06004](https://doi.org/10.21272/jnep.15(6).06004)

PACS number: 84.40 Ba

1. INTRODUCTION

The 5th generation of wireless technology has evolved from the 4th generation of wireless technology, and it promises to provide massive worldwide connectivity. 5G is designed to deliver higher data rates, ultra-low latency, higher reliability, higher capacity, wider coverage, and a better user experience compared to the previous generations of wireless systems [1, 2]. The Massive multiple-input-multiple-output (mMIMO) antennas and beamforming are the two technologies employed in 5G wireless networks to improve coverage, capacity, and reliability.

An antenna element designed for beamforming mMIMO antenna array is required to have a compact size, broad bandwidth, and dual polarization. The dual-polarized antenna is capable of mitigating multipath fading, reducing the size and number of antennas, and enhancing the channel capacity [2]. The increasing complexity of antenna systems in mMIMO and beamforming scenario have made conventional testing methods redundant. Now, novel over-the-air (OTA) test methods are being deployed for 5G and beyond wireless systems. This means that the device under test (DuT) will not be physically connected to the test equipment during testing.

Moreover, millimeter-wave (mmWave) bandwidths will be utilized by the 5G communication equipment for increased data speeds [3]. The testing at mmWave frequency bands is a challenge. The millimeter-wave (mmWave) devices using massive antenna arrays cannot be tested using cables as adding a connector to each antenna element is not feasible. Also, radio transceivers and antenna systems will be integrated into a single chip, leaving no space for radio frequency (RF) connectors [4].

In addition, higher frequency bands are associated with higher path loss. Beamforming is an effective technology implemented in multiple-input and multiple-output (MIMO) antenna systems to reduce these path losses. But measuring the performance of MIMO antennas in beamforming scenarios is difficult due to inaccuracies of power amplifiers and cable loss calibration. Moreover, the measurement time is also extended [5]. Thus, cabled methods must be abandoned.

To address these measurement challenges, OTA testing techniques are being investigated for the upcoming generations of mobile systems. 5G and beyond wireless communication will make use of multi-antenna arrays, which will create multiple beams and dynamically guide them in the appropriate directions using variations in the phase and amplitude of the signal delivered to each antenna element in an antenna array [6]. Multi-element antennas will be used in the sub 6 GHz as well as mmWave frequency bands.

A method of OTA interface is needed because base stations will employ a significant number of antenna elements to create many beams. For all of these beams, it is necessary to lock the 5G base station (gNB) downlink (DL) and attach multiple user equipment (UEs) on the uplink (UL) to make throughput and mobility measurements. Over-the-air (OTA) test techniques must be used in such a case. For testing RF performance (a minimum level of signal quality), demodulation (throughput performance), and radio resource management (handover, mobility, and initial access), OTA testing will be necessary [4].

The components of an OTA test technique include a chamber enclosure, probe antennas, and test tools for signal analysis. The chamber offers a protected setting

*spermvir2022@gmail.com

†F.H.Ali@sussex.ac.uk

for the controlled measurement of signals with a specific power and direction [4]. This article stipulates that the antenna for OTA testing must have wideband, linear polarization, and isolation features. For each test frequency, a narrowband antenna can be utilized. This approach, however, is not very practical because many antennas are needed to cover all of the test frequencies.

Using a wideband antenna to cover all the test bands is the more practical method. The antenna must be able to accommodate a broad range of frequency spectrums to be useful in ultra-wideband (UBW) technology. At UBW frequencies, the traveling-wave antennas have been proven to work satisfactorily. The traveling-wave antennas include horn antennas, dielectric rod antennas, and tapered slot antennas that can be utilized as wideband antennas to cover all required test bands [7]. The Vivaldi antenna, a tapered slot antenna with a wide bandwidth, symmetric radiation patterns in both co- and cross-polarization at microwave frequencies, and acceptable time domain behavior [8, 9], are the characteristics that make this antenna the best choice for this project. In addition, the Vivaldi antenna is the perfect option for the work being considered because of its low cost and simple fabrication method. The antenna with a small gain will be sufficient for OTA measuring needs because the distance between the DuT and the probe antenna is not too wide.

According to the authors, this antenna is the first of its kind in size, cost, frequency range, and application. The fundamentals of OTA testing are covered in part 2 of this study. In section 3, the design process for the construction of the dual-polarized Vivaldi antenna is described. In section 4, the conclusion is provided.

2. OVERVIEW OF OVER-THE-AIR TESTING

The massive MIMO integrated base stations are a fundamental requirement for capacity and throughput enhancement in 5G wireless technology at both sub-6GHz and mmWave frequency bands. The omission of RF test ports and the dynamic beamforming in massive MIMO scenarios make OTA testing inevitable for 5G deployment [10]. OTA testing includes testing and validation of MIMO and beamforming. Both MIMO and beamforming are implemented through electrically steerable antenna arrays [11]. Beamforming implementation calls for multi-element antenna arrays. Beam steering requires precise control over the signal phase that is applied to each antenna element. Using massive antenna element arrays, narrow beams can be produced [11].

Controlling the MIMO link between the transmitter and receiver is crucial to the 5G radio channel's functionality. A MIMO link should have a minimal correlation between the various data streams from the transmitting antennas to the receiving antennas. OTA testing is required because of the potential for substantial variations in the air interface, which have a considerable impact on radio link performance [11].

Massive MIMO active antenna systems enable fast communication but also complicate testing for 5G mobile systems [12]. Radiofrequency systems and antennas will function as a single physical unit with the implementation of mmWave frequencies. The performance of integrated solutions combining amplifiers, phase shifters, modems, and antennas in a single multilayer PCB chip

is crucial to the deployment of 5G infrastructure, whether it operates at sub-6 GHz (FR1) or mmWave (FR2) [10].

OTA test methods can be categorized as Conformance tests and Performance tests. Conformance tests are critical and include connecting devices to wireless test systems [13]. These tests yield minimum-level signal quality (RF transmission and reception), data throughput (demodulation), and radio resource management (mobility, handover, and initial access) [4]. 3GPP TR 38.810 [14] approved the following three OTA test methods:

(I) Direct Far Field (DFF). In this test method, the measurement antenna is kept in the far field, which starts at $2D^2/\lambda$, where D is the diameter of the radiating element and λ is the wavelength. In this region, the spherical waves transition into plane waves. This method is capable of measuring multiple signals with different angles of arrival (AoA) as it can accommodate multiple antennas [12, 13]. However, it can lead to an extended test range at mmWave frequencies [13]. This method is suitable for sub-6 GHz measurements.

(II) Indirect Far Field (IFF). Using a parabolic reflector to collimate the signals from the probe antenna, this technique condenses the amount of space needed to produce a far-field scenario [13, 14], and the setup is called Compact Antenna Test Range (CATR) [13, 15]. This method seems suitable for mmWave 5G OTA testing but it has the drawback of not providing multiple frequency ranges [14].

(III) Near-Field to Far-Field Transformation (NFTF). This technique involves first measuring the device under test (DuT) in the near field and then using the Fast Fourier Transform (FFT) to produce the far-field characteristics from the near-field measurements [13]. Due to the additional computations required, this method is the slowest of the three [12]. This approach exhibits testing deficiency in real-time device operation [14].

The essential OTA metrics include effective isotropic radiated power (EIRP), total radiated power (TRP), total isotropic sensitivity (TIS), effective isotropic sensitivity (EIS), spectrum emission mask (SEM), adjacent channel leakage ratio (ACLR), and error vector magnitude (EVM) [10, 16]. OTA solutions are developing quickly and playing a significant role in the verification process. To evaluate the 5G wireless systems in a real environment and avoid expensive field tests, OTA test systems simulate the multipath radio environments in a predictable, repeatable, and reliable manner [17]. OTA tests can enhance device design and hasten the rollout of 5G.

3. ANALYSIS AND DESIGN OF THE ANTENNA

A single antenna element is first designed, and subsequently, the design is expanded to include two antenna elements operating in dual-polarized mode. CST microwave studio is used to design, simulate and optimize the Vivaldi antenna. The proposed antenna is modeled with a view to achieving the following specifications given in Table 1.

The design of the antenna depends heavily on the dielectric material. The main factors that must be taken into consideration because they affect how well the antenna performs are thickness and dielectric constant.

Table 1 – Desired Antenna Parameters

No	Parameters	Values
1	Antenna size	90 × 90 × 90 mm ³
2	Frequency range	1.4 GHz – 6 GHz
3	Return loss	> 10 dB
4	Polarization	Linear
5	Radiation pattern	Peak gain in boresight
6	Gain	0 – 10 dBi
7	Cross Polarization	> 20 dB
8	Physical connection	Two SMA connectors (one per connection)
9	Cost	Low cost

Reduced antenna size and simplified fabrication is achieved by using substrate materials with high dielectric constant [18]. Such dielectric materials, however, cause the antenna's radiation efficiency and bandwidth to deteriorate [19]. The substrates with low dielectric constant and high thickness offer a large bandwidth, increased radiation efficiency, and efficient design at the expense of size [18, 20]. The design utilizes the substrate material Rogers RO4350B, which has a thickness of 0.5 mm, a dielectric constant of 3.48, and a dissipation factor ranging from 0.0031 to 0.0037.

The availability of the dielectric material and the proposed antenna's cost specifications are other important considerations in the selection of Rogers RO4350B. At the outset of the design process, the substrate needs to be carefully chosen based on the requirements of the antenna. The selection of an appropriate feeding technique is also very important in designing the antenna. Microstrip to slot line feed is chosen to excite the antenna because of its planar structure, ease of implementation, and widespread use in tapered slot antennas. The radial stub is used at the end of the microstrip for broadband operation.

A microstrip feed line is built on one side of the substrate material and a copper plate with an etching of 0.035 mm thickness on the other. The design methodology involves studying the various antenna parameters, analyzing their impact on the performance of the antenna through simulations, and then optimizing them to obtain the best design that could satisfy the requirements of a specific application. This is because there is no concrete and well-defined procedure available for designing the antenna. Vivaldi antenna and its parameters are shown in Fig. 1.

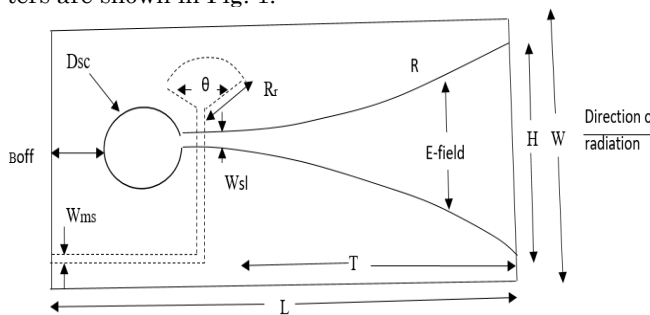


Fig. 1 – Vivaldi Antenna Geometry and Parameters

A description of the Vivaldi antenna parameters is given in Table 2.

Table 2 – Vivaldi Antenna Parameters

No	Notation	Parameters
1	L	Antenna length
2	W	Antenna width
3	H	Aperture size
4	R	Taper rate
5	T	Taper length
6	B_{off}	Backwall offset
7	D_{sc}	Circular cavity diameter
8	W_{sl}	Slotline width
9	W_{ms}	Microstrip width
10	R_r	Radial stub radius
11	θ	Radial stub angle

By using the mathematical equations given in the literature, antenna dimensions can be calculated. The width and length of the antenna can be calculated from the equation [21].

$$W = L = \frac{c}{fL} \sqrt{\frac{2}{\epsilon r + 1}}, \quad (1)$$

where L is the length of the antenna, W is the width of the antenna, C is the free space velocity of light, fL is the minimum frequency of operation, and ϵr is the dielectric constant. The maximum and minimum aperture size of the antenna is calculated using the equations [22].

$$\lambda_g = \frac{c}{f_{min} \sqrt{\epsilon r}}, \quad (2)$$

where λ_g is the guide wavelength, C is the speed of light, f_{min} is the minimum frequency, and ϵr is the dielectric constant. The maximum opening width or aperture size is given by

$$W_{max} = \frac{\lambda_g}{2}. \quad (3)$$

The minimum opening width is given by

$$W_{min} = \frac{c}{f \sqrt{\epsilon r}}, \quad (4)$$

where f is centre frequency.

The taper rate of the Vivaldi antenna is computed using the equation [23, 24].

$$y = \pm(C_1 e^{Rx} + C_2), \quad (5)$$

where C_1 and C_2 are constants given by $C_1 = \frac{y_2 - y_1}{e^{Rx_2} - e^{Rx_1}}$ and $C_2 = \frac{y_1 e^{Rx_2} - y_2 e^{Rx_1}}{e^{Rx_2} - e^{Rx_1}}$. R defines the opening rate of exponential taper and determines the beamwidth of the Vivaldi antenna. (x_1, y_1) defines the coordinates of origin and (x_2, y_2) defines the coordinates of flare end points.

According to conventional knowledge of Vivaldi antenna design, the length of the antenna should be greater than one wavelength at the lowest design frequency [20], and the width should be half a wavelength at the lowest operating frequency. This information, combined with the mathematical equation in (1), results in length and width dimensions that do not meet the size requirements set forth for this antenna. The compact size is the primary design objective for this antenna, thus its length and width could not be extended above 90 mm. As a result, significant parametric study and

analysis are required for this antenna. The return loss of an antenna, which determines its operational bandwidth, is the most crucial criterion for wideband antennas. The amount of radio frequency power that the antenna reflects rather than accepts is known as return loss. The permitted operating level is 10 dB of return loss, which translates to 10% of the power reflected and 90% of the power radiated by the antenna. The design process intends to develop an antenna that could meet the 10 dB criterion over the whole 1.4 – 6 GHz operating frequency. The width of the microstrip feed line is finetuned to obtain the input impedance of 50 Ω . By progressively and continually changing the characteristic impedance of the tapered microstrip feed line along its length, the impedance matching with the antenna is achieved. The initial value of aperture size is calculated using the equations given in (3) and (4). The initial taper rate value is derived from equation (5) in MATLAB software. The starting stub angle is chosen to be 60 degrees. The CST MWS software is used for numerical simulation of the antenna configuration in the time domain solver after declaring the initial values of the antenna parameters. A thorough parametric analysis of several antenna characteristics is conducted, and these parameters are then tuned to provide the best possible antenna performance while meeting the design performance.

3.1 Parametric Study and Analysis

Increasing the antenna's length and width increases its bandwidth, especially at the lowest working frequencies. The reduction in width and length dimensions of the antenna reduces the system bandwidth. Increased aperture size or mouth opening enhances antenna performance in the lower frequency range, enabling the required band's lowest frequency to be attained. With changes in aperture size, the antenna's high-frequency return loss response nearly stays constant. Antenna impedance and free space impedance are matched by aperture size. The choice of the aperture size must therefore strike a compromise between improving the return loss in the lower frequency range and achieving impedance matching in the higher frequency range.

The backwall offset is an additional metallization that is added behind the circular cavity to prevent the abrupt termination of currents. The lower values of backwall offset are seen to deteriorate the performance of the antenna at lower frequencies. The higher frequencies show little variation with the variation in the backwall offset values. The reduction in cavity diameter results in poor return loss of the antenna at the lower frequencies. Higher cavity diameter improves the antenna bandwidth. The variation in slot line width has more impact on the higher frequencies in the designated frequency range than the lower frequencies. The decrease in slot line width results in improved return loss performance of the antenna at higher frequencies of the spectrum. An increase in slot line width improves low-frequency transmission. The width of the slot line has to be large enough to realize an orthogonal structure because the antenna is to be used in dual-polarized mode. Hence, a trade-off in the parametric value of slot line width is achieved.

The taper rate of the slot line is observed to impact

the mid-band frequencies of the desired band. The decrease in taper rate shows considerable improvement in the center frequencies of the frequency range. However, the decrease in taper rate degrades the antenna performance at the lower frequencies. The literature on designing Vivaldi antennas states that the taper length is typically half of the wavelength at the lowest frequency in the desired band for efficient energy radiation. The antenna's taper length is optimized with the necessary antenna dimensions in mind because increasing the taper length would lengthen the antenna even though it is seen that a longer taper length would boost performance. Again, a trade-off is considered.

The stub radius and stub angle are optimized for optimum antenna performance after the effects of these parameters on the operational bandwidth of the antenna are investigated. The optimized antenna parameters obtained from parametric analysis and CST simulations for the best possible antenna performance are shown in Table 3.

Table 3 – Optimized parameters

No	Parameters	Values
1	L	86 mm
2	W	90 mm
3	H	51 mm
4	R	0.063
5	T	66 mm
6	B_{off}	4 mm
7	D_{sc}	12 mm
8	W_{sl}	1 mm
9	W_{ms}	1.4 mm
10	R_r	5 mm
11	θ	900

3.2 Simulated Antenna Prototypes

The designed single-element Vivaldi antenna is seen in Fig. 2.



Fig. 2 – Single Element Vivaldi Antenna

The connectors should be suitable to send a microwave signal to the transmission line. For the SMA connectors – which are used to link the microwave energy – to grasp the edge of the circuit board securely and prevent gaps, the feed structure has to be coplanar. Due to the mismatch in dimensions between the contactor contact and substrate thickness, there may be a significant amount of energy that is reflected when it comes to thin substrates [25]. To avoid these problems, a coplanar to microstrip transition is constructed. The ground plane on the substrate's back and the coplanar waveguide (CPW) ground are connected using metallic via holes.

Differential port feeding is used to excite the coplanar waveguide structure. Differential feeding involves

feeding 180-degree phase-shifted signals with equal amplitude to the opposing ports. Fig. 3 depicts the front and back view of the designed antenna with CPW to microstrip transition.

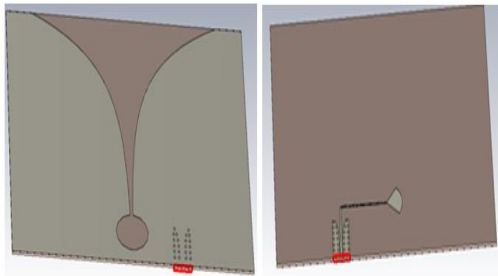


Fig. 3 – Front and Back View of the CPW-Microstrip Vivaldi Antenna

Fig. 4 illustrates a dual polarized (horizontal and vertical) Vivaldi antenna made out of the two Vivaldi antenna elements (VAE) incorporated into a single orthogonal structure. To prevent feeding lines from crossing each other and causing mutual coupling of microwave radiation, one antenna element is moved ahead of the other, creating a dual-polarized antenna with an offset between the two antenna elements.

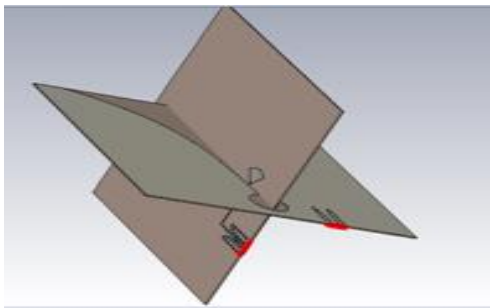


Fig. 4 – Dual Polarized Vivaldi antenna with offset

Another dual-polarized antenna prototype is created without offset. Comparing the outcomes of the two prototypes is intended to help determine which antenna produces more precise findings. This antenna is created by cutting out two equal-length rectangular slots in the ground plane at the back of each antenna's circular cavity as shown in Fig. 5.

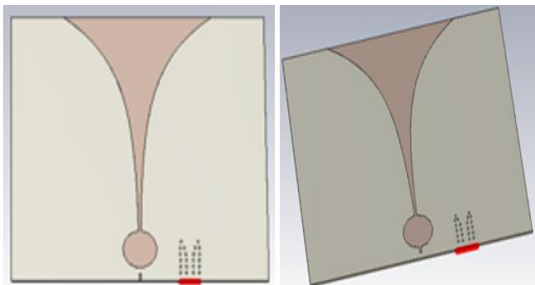


Fig. 5 – Single polarized Vivaldi antennas with cut-outs

Fig. 6 shows the dual-polarized Vivaldi antenna without offset between the antenna elements. The feeding lines are made to pass through the slot line at different positions to prevent them from overlapping each other in dual polarization configuration.

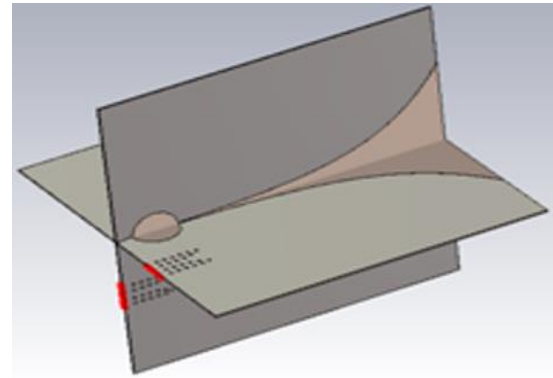


Fig. 6 – Dual Polarized Vivaldi Antenna without Offset

3.3 Simulation Results and Discussions

Fig. 7 shows simulated return loss (S_{11} , S_{22}) and cross-polarization discrimination (S_{21} , S_{12}) of dual-polarized Vivaldi antenna with offset.

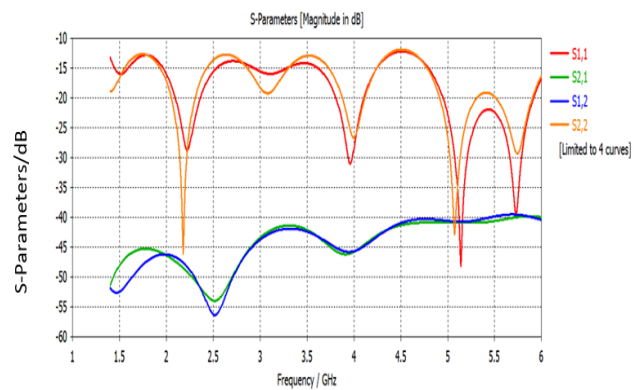


Fig. 7 – Return loss & Cross-polarization Rejection of Antenna with Offset

Fig. 8 shows the simulated return loss (S_{11} , S_{22}) and cross-polarization rejection (S_{21} , S_{12}) of the dual-polarized Vivaldi antenna without offset.

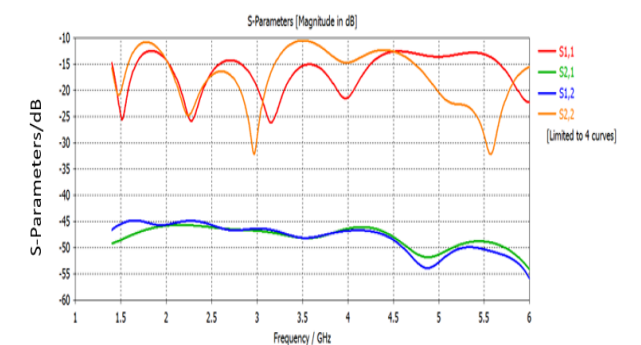
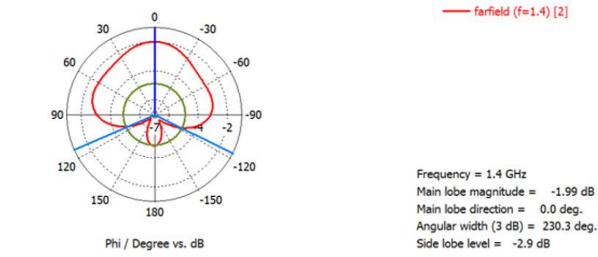
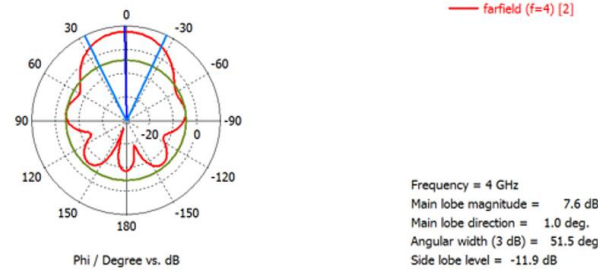


Fig. 8 – Return loss & Cross-polarization Rejection of Antenna without Offset

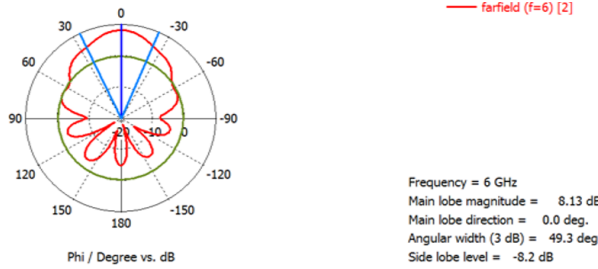
The simulation results demonstrate that the return loss in both prototypes exceeds 10 dB, the threshold that this antenna requires to function as a wideband antenna and cover the entire targeted band of frequencies. S_{11} indicates the return loss when the antenna is excited at port 1, while S_{22} represents the return loss when the antenna is excited at port 2.



(a)



(b)



(c)

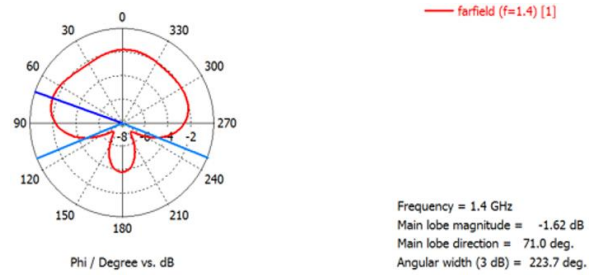
Fig. 9 – 2-D Radiation Pattern (a) 1.4 GHz, (b) 4 GHz, (c) 6 GHz of the antenna with offset

The simulations also show that the cross-polarization rejection is higher than 20 dB, which is required of this antenna to produce optimal results. A polarization that is orthogonal to the preferred polarization is referred to as cross-polarization. Vertical polarization is cross-polarization if the fields coming from the antenna are horizontally polarized and vice versa. The cross-polarization rejection measures the rejection of orthogonally polarized transmissions and reflects the polarity of an antenna element. S_{21} and S_{12} represent the cross-polarization discrimination when the antenna is excited at port 1 and port 2 respectively.

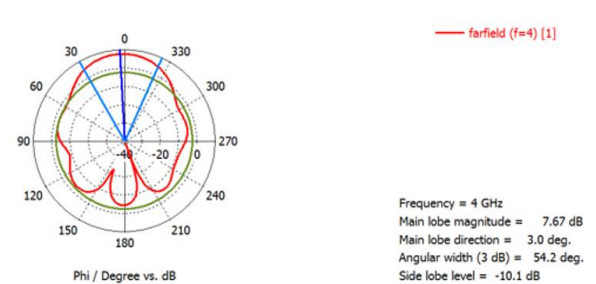
The radiation pattern, which depicts the distribution of radiated energy in space, is a significant and fundamental characteristic of the antenna. 2-D radiation patterns of the simulated antenna at 1.4 GHz, 4 GHz, and 6 GHz for dual-polarized Vivaldi antenna with offset are shown in Fig. 9.

Fig. 10 shows the simulated radiation patterns of the dual-polarized Vivaldi antenna without offset at 1.4 GHz, 4 GHz, and 6 GHz.

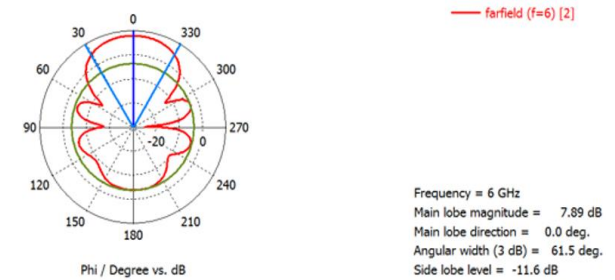
The results of 2-D radiation pattern simulations for the dual-polarized Vivaldi antenna with an offset demonstrate that the peak gain is in the direction of the boresight over the target band, satisfying the criterion of the proposed antenna. However, simulations for the dual-polarized Vivaldi



(a)



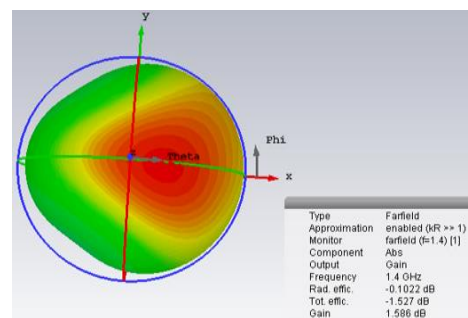
(b)



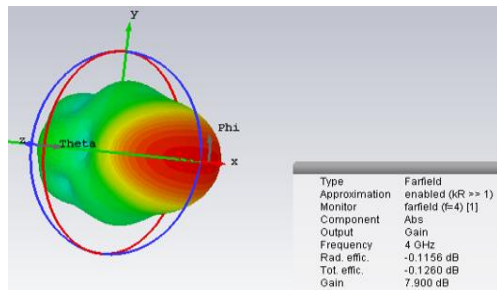
(c)

Fig. 10 – 2-D Radiation Pattern (a) 1.4 GHz, (b) 4 GHz, (c) 6 GHz of the antenna without offset

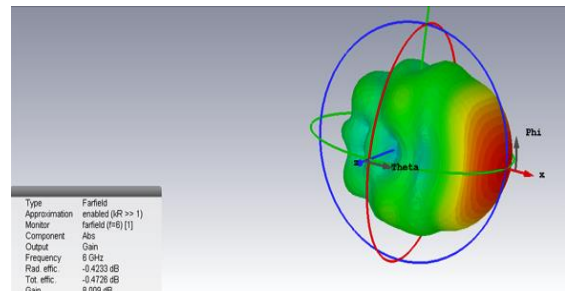
antenna without an offset show that the peak gain deviates from the boresight direction at the lower components of the frequency range. Due to the antenna's small size, radiations at the lowest frequency part of the desired frequency spectrum are reflected, which is the source of this discrepancy. By using a metal plate at the back of the antenna to absorb reflections, this issue can be addressed. Yet, the antenna displays the desired far-field 2-D radiation patterns for all other frequencies in the intended frequency band. Fig. 11 shows the simulated gain, radiation efficiency, and total efficiency at 1.4 GHz, 4 GHz, and 6 GHz for dual-polarized Vivaldi antenna with offset in 3D radiation patterns.



(a)



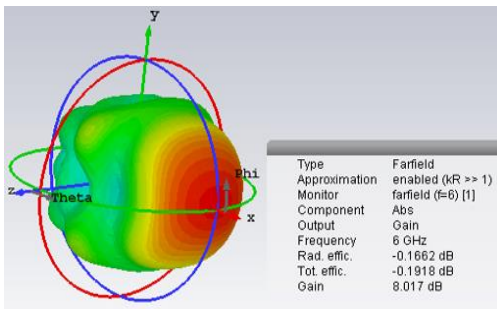
(b)



(c)

Fig. 12 – 3-D Radiation Pattern (a) 1.4 GHz, (b) 4 GHz, (C) 6 GHz of the Vivaldi antenna without offset

The simulated antenna gains are 1.586 dB, 7.900 dB, and 8.017 dB at 1.4 GHz, 4 GHz, and 6 GHz, respectively for dual-polarized Vivaldi antenna with offset, which agree with the antenna's specified gain requirements. With a dual-polarized Vivaldi antenna without offset, the simulated antenna gains are -1.755 dB, 7.527 dB, and 8.009 dB at 1.4 GHz, 4 GHz, and 6 GHz, respectively. At the lowest frequency of 1.4 GHz, it is observed that the antenna without offset does not perform as well in terms of antenna gain and radiation pattern as the antenna with offset. However, both simulated antenna prototypes have performed admirably over the majority of the necessary frequency range and have complied with the antenna's requirements.



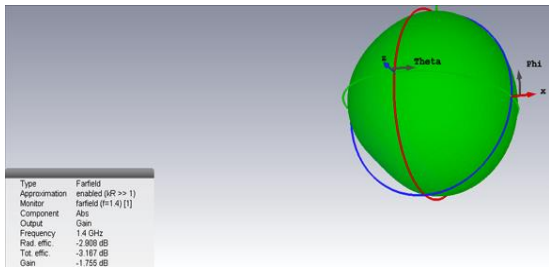
(c)

Fig. 11 – 3-D Radiation Pattern (a) 1.4 GHz, (b) 4 GHz, (c) 6 GHz of the Vivaldi antenna with offset

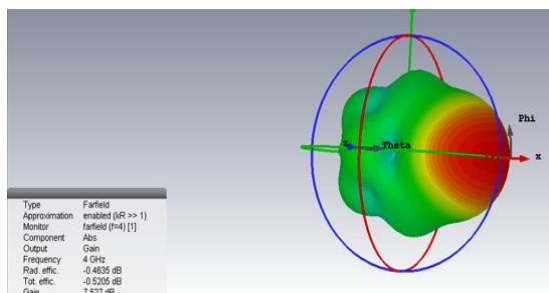
Fig. 12 depicts the simulated gain, radiation efficiency, and total efficiency at 1.4 GHz, 4 GHz, and 6 GHz for dual-polarized Vivaldi antenna without offset in 3D radiation patterns.

4. CONCLUSION

This study describes a dual-polarized Vivaldi antenna with broad-bandwidth and high isolation for OTA measurements of 5G base stations. The antenna is designed to resonate over a sub-6 GHz frequency spectrum. Two dual-polarized antenna prototypes are designed and simulated. Both prototype designs achieve the 10 dB criterion for wideband operation over the entire intended frequency range. XPD is found to be greater than 20 dB over all the frequencies in the desired frequency range. The simulation results show that the antennas perform with the desired gain and radiation pattern. The antenna is modeled on a 0.5 mm thick dielectric material. This culminates in the development of a highly thin and light antenna. The goal of this research is to demonstrate that it is feasible to design an electrically small and inexpensive antenna that can test 5G New Radio over-the-air while covering the whole sub-6 GHz frequency band. We anticipate that the actualized antenna will satisfy the design requirements. The fabrication errors may be the only reason for the divergence from the simulated outcomes.



(a)



(b)

REFERENCES

1. A. Gupta, R.K. Jha, *IEEE Access* **3**, 1206 (2015).
2. C.H. Le Thi, S.X. Ta, X.Q. Nguyen, K.K. Nguyen, C. Dao Ngoc, (2021), *International Journal of RF and Microwave Computer-Aided Engineering* **31** No 5, e22615 (2021).
3. N. Ojaroudiparchin, M. Shen, G.F. Pedersen, *23rd Telecommunications Forum Telfor (TELFOR)*, 587 (2015).
4. Keysight, "The What, When, Where, and Why of 5G NR OTA Testing | Keysight Blogs," The What, When, Where, and Why of 5G NR OTA Testing | Keysight Blogs, Feb. 22, 2023. [online]. Available: https://blogs.keysight.com/blogs/inds.entry.html/2018/11/19/the_what_when_where-A3CH.html.
5. G.-H. Jeon, P.A. Dzagbletey, J.-Y. Chung, *Journal Of Electromagnetic Engineering And Science* **21** No 3, 201 (2021).
6. Nadder Hamdy, M., 2020. Beamformers Explained. [online] Commscope.com. Available at: <https://www.commscope.com/globalassets/digital/542044-Beamformer-Explained-WP-114491-EN.pdf>.
7. G. Adamiuk, T. Zwick, W. Wiesbeck, *IEEE Trans. Anten. Propag.* **58** No 2, 279 (2010).
8. G. Adamiuk, T. Zwick, W. Wiesbeck, *MIKON 2008 - 17th International Conference on Microwaves, Radar and Wireless Communications*, 1 (2008).
9. Erdogan, Y 'Parametric Study and Design of Vivaldi Antenna and Arrays'. 2009 [Online] Available at: <https://open.metu.edu.tr/bitstream/handle/11511/18522/index.pdf>.
10. B. Derat, C. Rowell, A. Tankielun, S. Schmitz, *Microwave Journal* **61** No 8, 96 (2018).
11. Doucette, "5G Testing Discussion Panel," Gap Wireless. <https://staging.gapwireless.com/tech/5g-testing-discussion-panel/>.
12. A. Khan, "Verifying 5G with OTA testing," Verifying 5G with OTA testing. <https://www.testandmeasurementtips.com/verifying-5g-with-ota-testing-faq>.
13. P. Hindle, *Microwave Journal* **62** No 3, 20 (2019).
14. Miguel Á. García-Fernández, EMITE Ingeniería S.L. and David A. Sánchez-Hernández, 'Challenges for Effective and Realistic 5G OTA Testing', *Microwave Journal*, 2019. [Online]. Available at: <https://www.microwavejournal.com/articles/31755-challenges-for-effective-and-realistic-5g-ota-testing>
15. J.S. Hurtarte, M. Wen, Over-the-Air Testing for mmWave Devices: DFF or CATR? *Microwaves & RF* [Online] Available from: <https://www.mwrf.com/technologies/test-measurement/article/21849577/overtheair-testing-for-5g-mmwave-devices-dff-or-catr>.
16. M. Gustafsson, T. Jämsä, M. Högberg, *2017 XXXII Ind General Assembly and Scientific Symposium of the International Union of Radio Science (URSI GASS)*, 1 (2017).
17. M. Belhabib, (2020) *International Journal of Future Computer and Communication* **9** No 1, 1 (2020).
18. Van Thuan Nguyen, Chang Won Jung, *International Journal of Antennas and Propagation* **2014**, 6 (2014).
19. Oluwafemi A. Plesanmi, and Charles U. Ndujiuba, *International Journal of Networks and Communications* **2** No 8, 37.
20. S. Shijina, R. Sareena, Shameer K. Mohammed, *IOSR Journal of Electronics and Communication Engineering (IOSR-JECE)*, 80.
21. M.Y. Perdana, T. Hariyadi, Y. Wahyu, *IOP Conference Series Material Science and Engineering* **180**, 012058 (2017).
22. N. Hamzah, K.A. Othman, London. In *Proceedings of the World Congress on Engineering, II*, WCE (2011).
23. J. Shin, D.H. Schaubert, *IEEE Trans. Anten. Propag.* **47** No 5, 879 (1999)
24. S. Lizhong, F. Qingyuan, *Proceedings of 2011 Cross Strait Quad-Regional Radio Science and Wireless Technology Conference*, 494 (2011).
25. M. El-Gibari, D. Averty, C. Lupi, Y.M. Hongwu Li, S. Toutai, *Ultra Wideband Communications: Novel Trends - Antennas and Propagation*, (2011).

Компактна ширококутова подвійно-поляризована антена для OTA-тестування нового радіо до 6 ГГц 5G

P. Singh¹, F.H. Ali²

¹ Department of Test and Measurement, Rohde & Schwarz., New Delhi, India

² School of Engineering and Informatics, University of Sussex., United Kingdom

Впровадження антенних решіток, формування променя та зв'язку на міліметрових хвилях у мережі 5G вимагає нового підходу до тестування радіопродуктивності пристроїв. Бездротове тестування є практичним рішенням для вимірювання радіопродуктивності бездротових систем нового покоління. У цьому документі представлено аналіз і дизайн подвійної поляризованої антени Vivaldi для бездротового тестування базової станції 5G для частотного діапазону від 1,4 ГГц до 6 ГГц. Розроблена антена складається з двох елементів, розташованих ортогонально. Змодельовано два прототипи антени Вівальді з подвійною поляризацією: одна зі зміщенням між елементами антени, а інша — без зміщення між елементами антени. Ширококутова антена в основному характеризується прийнятним коефіцієнтом відбиття (S11) у бажаній робочій смузі пропускання. Результати моделювання показують, що S11 менше -10 дБ у діапазоні частот від 1,4 до 6 ГГц в обох прототипах. Симулятор CST Studio Suite EM використовується для створення та моделювання запропонованої антени з використанням підкладки Rogers RO4350B, яка має загальний розмір 86 × 90 × 0.5 мм³. Запропонована антена буде використовуватися на стороні UE всередині беззехової камери для тестування базової станції 5G по повітрю щодо пропускну здатності та мобільності. Компактний розмір і низька вартість є ключовими характеристиками цієї антени. Низька вартість досягається використанням дешевого діелектричного матеріалу.

Ключові слова: Формування променя, Подвійна поляризація, Ефірне тестування, Діаграма спрямованості, Зворотні втрати, Антена Vivaldi.